Mean-field theories of cuprate superconductors: A systematic analysis

M. Grilli
Department of Physics, University of Rome la Sapienza, I-00185 Rome, Italy

B. G. Kotliar
Serin Laboratory of Physics, Rutgers University, P.O. Box 819, Piscataway, New Jersey 08854

A. J. Millis
AT&T Bell Laboratories, 600 Mountain Avenue, Murray Hill, New Jersey 07974
(Received 30 November 1989)

The lattice Anderson model believed to be relevant to high-temperature superconductors and heavy-fermion metals exhibits a variety of different behaviors, including mixed-valence, heavy-fermion, and Mott-insulating states. We determine, via an auxiliary-boson mean-field theory, the parameter regimes in which these behaviors exist. For the two-dimensional CuO_2 Anderson model we calculate the susceptibility and quasiparticle plasma frequency. By comparing these to specific-heat, susceptibility and optical data for high-T_c superconductors, we determine that the materials are in a regime controlled by proximity to a Mott transition and that magnetic correlations play an essential role.

I. INTRODUCTION

Models involving a band of weakly correlated fermions coupled to a band of strongly correlated, nearly localized fermions have received substantial attention from condensed-matter theorists because of their probable relevance to the high-T_c oxide superconductors and to heavy-fermion metals. These models display a variety of phenomena, including conventional or light-mass Fermi-liquid behavior, large-mass heavy-fermion behavior, and a metal-insulator transition to an insulating magnetic state. Particular limits of these models have been extensively studied, but to our knowledge there has been no systematic analysis of the various regimes and the crossovers between them. In this paper we perform a part of this systematic analysis using an auxiliary boson mean-field-theory description of the "CuO_2" models which are widely supposed to describe the high-T_c superconductors. The mean-field theory is believed to provide a qualitatively correct description of the Fermi-liquid behavior that occurs when intersite magnetic interactions in the strongly correlated band may be neglected. Behavior of the non-Fermi-liquid regime is not yet well understood. After elucidating the various parameter regimes and the crossovers between them, we attempt to determine which regimes are relevant for the high-T_c superconductors by evaluating our expressions using model Hamiltonian parameters determined from local density calculations and by interpreting experimental data. We conclude that formulating a theory which takes proper account of intersite magnetic correlations is crucial.

The rest of the paper is organized as follows. In Sec. II we give a general discussion of the various possible regimes and we define the important parameters. We also discuss the mean-field theory and its probable domain of applicability and review other work. In Sec. III we solve a simple one-dimensional model in detail, displaying the different regimes and the parameters governing the crossovers. In Sec. IV we consider a more realistic two-dimensional model. Calculations in this model require much more extensive numerical work, so we confine ourselves to a few representative sets of parameters, including those proposed on the basis of local-density calculations. In Sec. V we consider the extent to which experimental data points to one parameter regime or another. Section VI is a conclusion. Readers uninterested in the details of the mean-field calculations may wish to consider only Secs. II, V, and VI and the figures. These sections discuss the principal results and their application to high-T_c superconductors and may be read independently of Secs. III and IV, in which the principal results are derived.

II. MODEL AND GENERAL DISCUSSION

We consider the canonical CuO_2 lattice shown in the upper part of Fig. 1. We include one d orbital at energy ε_d^0 on the Cu site and one p orbital at energy ε_p on each O site. We assume a hybridization matrix element t_{pd} between adjacent Cu d and O p orbitals and a hybridization matrix element t_p between adjacent O p orbitals. The phases are chosen appropriately for Cu $d_{x_2-y_2}$ and $O_{p\sigma}$ orbitals.

We assume a hole notation, so that the vacuum is the state in which all orbitals are fully occupied. It is now widely accepted[1] that the energy cost to doubly occupy the Cu site with holes, U_{dd}, is approximately 8 eV, larger than other energies in the problem. We assume $U_{dd}=\infty$.

One important parameter is E_g, the negative of the energy of the Cu d level measured relative to the bottom of

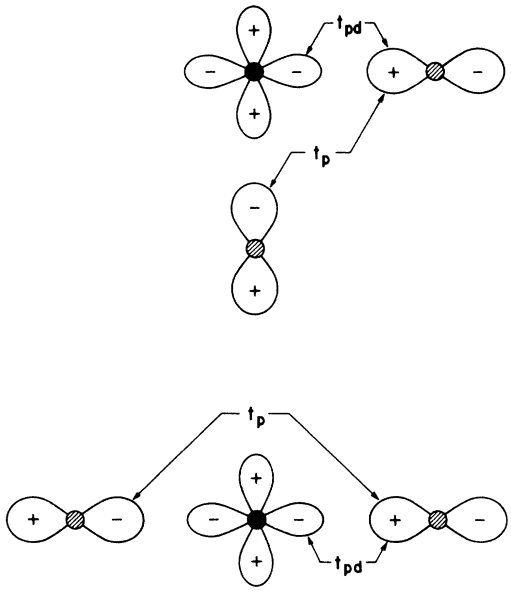

FIG. 1. Sketch of unit cell with orbitals and hopping matrix elements indicated: (top) unit cell for physically relevant CuO_2 lattice; (bottom) unit cell plus oxygen from neighboring cell for one-dimensional model solved in Sec. III.

the oxygen band. In the CuO_2 model defined in Fig. 1 the lowest state in the oxygen band occurs at the zone corner and has energy $\varepsilon_p = 4t_p$, so

$$E_g = \varepsilon_p - 4t_p - \varepsilon_d^0 \ . \tag{2.1}$$

Another important parameter is the doping δ defined in terms of the number of holes per unit cell n_h via

$$\delta = n_h - 1 \ . \tag{2.2}$$

The model with $t_p = 0$ has been extensively studied.[2,3] It has been determined that if E_g/t_{pd} is sufficiently large, $E_g > E_g^c$, the model is a Mott insulator at half-filling, $\delta = 0$. E_g is the gap in the Mott insulating phase. An important energy scale in the insulating phase is the antiferromagnetic exchange coupling J.

One may also consider the energy cost to doubly occupy an O site with holes, U_{pp}. In the real materials U_{pp} may be as large as 4 eV. However, in the situations of interest to us in this paper, the occupancy of an oxygen site is small, ranging from $\sim\delta/2$ in the $E_g \gg t_{pd}$ limit to $\sim\frac{1}{4}$ when $E_g = 0$ (when $E_g = 0$ the total Cu and O occupancies are equal and there are two O sites per unit cell). Thus the probability of an O site being doubly occupied by holes is small, so that the term involving U_{pp} may be neglected. We set $U_{pp} = 0$ throughout.

If $E_g > E_g^c$ and $\delta < 0$, i.e., with electron doping of the insulating state, one can eliminate the O states by perturbation theory and the model clearly maps onto a one-band Hubbard model. For this model it is believed[4] that the effective Fermi energy E_F^* is proportional to δ as $\delta \to 0$ provided $E_F^* > J$. If $E_F^* < J$, more exotic behavior occurs.[5-7]

If $E_g > E_g^c$ and $\delta > 0$ the situation is not so clear, for the added holes must reside on the O sites. Rice and Zhang[2] have argued that if one extra hole were added to the Mott insulating state, it would be bound into a singlet with a spin on a Cu site thus eliminating one Cu spin just as if an electron had been added. The energy of the bound state would be below the bottom of the oxygen band because the virtual hybridization between the O hole and the Cu must lower the energy. Rice and Zhang[2] speculated that at finite concentration of added holes these bound states would form a band lying below the bottom of the oxygen band. They estimated that the energy gain per hole and the effective hopping matrix element were of order t_{pd}^2/E_g, so that as long as one confined attention to sufficiently small δ and to energies less than t_{pd}^2/E_g the model would map onto a one-band Hubbard model, as in the case $\delta < 0$. Kotliar, Lee, and Read[3] solved the $t_p = 0$ model using a "slave-boson" mean-field technique. Among other results, they found that if at $\delta = 0$ the model is an insulator, then at $\delta > 0$ a quasiparticle band of Fermi energy $E_F^* \sim \delta t_{pd}^2/E_g$ was split off from the oxygen band by an energy $\sim t_{pd}^2/E_g$. The quasiparticle band is precisely the slave-boson mean-field theory representation of the singlet band proposed by Rice and Zhang. Kotliar, Lee, and Read discussed the physical interpretation of the quasiparticle states and calculated the spin and charge susceptibilities, assuming that the model was in the Fermi-liquid regime. Their criterion for Fermi-liquid behavior is $\delta t_{pd}^2/E_g > J$. In the regime $J > \delta t_{pd}^2/E_g$, they expect different physics.

In this paper we extend the above analysis to the case of finite oxygen-oxygen hopping, $t_p \neq 0$. There are several motivations. One is that various calculations of model Hamiltonian parameters have determined that t_p/t_{pd} is not small. Another is that the physical picture proposed by Rice and Zhang[2] must break down for sufficiently large t_p and δ. In this limit one has a large number of itinerent carriers coupled to local moments, as in the heavy-fermion metals. *In this case the quasiparticle band appears as a scattering resonance in the itinerant band rather than a set of bound states below the itinerant band.* The effective Fermi energy is exponentially small, exponentially sensitive to δ, and decreases as δ increases. Specifically,

$$E_F^* \sim t_p \exp\{-[t_p(E_g + 4\delta t_p)/t_{pd}^2]\} \ .$$

In this case E_F^* is often referred to as the "Kondo temperature" and denoted T_K. The heavy-Fermion state has been extensively studied on the assumption $E_F^* > J$.[8-10] The heavy-Fermion state is nonmagnetic. Again the large mass or low E_F^* is due to the quenching of the spin entropy on the scale of E_F^*. As pointed out years ago by Doniach,[11] in the limit $J > E_F^*$ one expects magnetic order in the local moments and light electron behavior in the conduction electrons. The crossover that occurs when $E_F^* \sim J$ is not understood.

Finally, we mention the intersite (p-d) Coulomb interaction, V. This interaction was introduced as a possible pairing mechanism of high-temperature superconductivity by Varma, Schmitt-Rink, and Abrahams.[12] Proper treatment of V may be essential for correct calculation of

the quasiparticle pairing interactions; however, these are beyond the scope of the present work. In the context of the present calculations the principal effect of V is to shift the value of the parameter E_g to $E_g'=E_g+2V$. The demonstration is given in the Appendix; elsewhere in the paper we assume V is included in E_g.

The CuO_2 model we have described has been intensively studied by many authors. We have already mentioned the work on the models with $t_p=0$ of Kotliar, Lee, and Read[3] and Rice and Zhang.[2] Newns, Rasolt, and Patinaik[13] have studied a set of parameters corresponding to $E_g<E_g^c$, allowing for a nonzero t_p and a finite U_{dd} but setting V and $J=0$. Balseiro *et al.*,[14] have studied a model with finite U_{dd} and a nonzero V but $J=0$, finding results similar to those of Kotliar, Lee, and Read.[3] Kim, Levin, and Auerbach[15] have considered a model without V or J, but with finite t_p, and have considered several different values of E_g. They calculated the Hall resistivity, and argued that the doping dependence of this quantity could be understood using the Fermi-liquid-based mean-field theories. Their calculation assumes that the correlations which produce insulating behavior at half-filling affect only the in-plane hopping, but not the between-plane hopping. This assumption appears to us not to be valid. More recently these authors have considered electron-phonon coupling in these models.[15] Castellani and Kotliar[16] considered a model with $t_p=0$ but $J\neq 0$ and discussed the transitions between the Fermi-liquid regime and some of the non-Fermi-liquid regimes that might be obtained.

In the present work we systematically examine the variation with t_p and J of the properties of the CuO_2 model, distinguishing several different regimes of behavior and giving the parameter values at which crossovers or transitions between them occur. Then, by calculating such physical quantities as the mobile carrier plasma frequency, the specific heat, and the susceptibility and comparing with experiment, we attempt to determine which parameter regimes are relevant for the high-T_c materials.

To perform the analysis we use the slave-boson mean-field-theory technique.[17] This technique has been extensively applied to the one impurity and lattice Kondo and Anderson problems, and has also been used to study several regimes of the CuO_2 models. It is believed to treat correctly the $U_{dd}=\infty$ constraint. The mean-field theory becomes exact in a large-N limit (N is a spin degeneracy) and even at finite N is known in the Kondo problem to give correctly (i.e., to leading logarithmic accuracy) the effective Fermi energy E_F^*, *provided* $E_F^*>J$. As t_p and $\delta\rightarrow 0$ with $E_g>E_g^c$ it gives results that agree (up to factors of order unity) with those of Rice and Zhang.[2] We believe therefore that the mean-field theory gives a reasonable estimate for the two energy scales, E_F^* and E_g^c, for various values of t_p, t_{pd}, and δ if J is sufficiently small.

In the slave-boson method one introduces an auxiliary boson field, $\hat{b}_i^\dagger$, which represents a Cu site with no holes. It is then necessary to rewrite the p-d hybridization as

$$(t_{pd}d_{i\sigma}^\dagger p_{j\sigma}\hat{b}_i+\text{H.c.})$$

In the mean-field theory one replaces $\hat{b}$ by its expectation value b. Because there is at most one hole per Cu, $b\leq 1$. A nonzero mean-field value of b represents coherent hybridization between p and d levels, so that the p and d holes combine to form a Fermi liquid. The hybridization is, however, reduced from the noninteracting value by correlation effects, which are represented by a value $b<1$. If $b=0$ then there is no coherent coupling between the Cu and O sites, so that the holes on the Cu sites will not directly participate, e.g., in the low-ω electrical conductivity. The interpretation of the boson field b has been discussed at greater length elsewhere.[8,9,17,18]

The other important element in the slave-boson method is the constraint $\sum_\sigma d_{i\sigma}^\dagger d_{i\sigma}+b_i^\dagger b_i=1$. This expresses the fact that on each Cu site the only allowed states are those with zero or one hole. The constraint is enforced with a Lagrange-multiplier field $\hat{\lambda}_i$, which in the mean-field theory is replaced by its expectation value λ (again assumed to be site independent). λ is conventionally rewritten as $\lambda=\varepsilon_d-\varepsilon_d^0$, thus defining ε_d, the quasiparticle d-level energy. ε_d is closely related to the Fermi energy and is also a convenient parameter to use in the solution of the mean-field theory.

In principle, intersite magnetic correlations are generated by the Hamiltonian given in Fig. 1. It is a defect of the slave-boson method that these magnetic correlations do not appear in the mean-field theory. An approximate method of incorporating these correlations is to add to the mean-field theory a term of the form $J\sum_{\langle ij\rangle}\mathbf{S}_i\cdot\mathbf{S}_j$ where $\mathbf{S}_i$ is the spin on Cu site i. This term may be treated, e.g., in one of the Hartree-Fock approximations devised in the context of resonating-valence-bond (RVB) theory.[19,20] We believe and will show below that this approximation gives a physically reasonable qualitative description of the effect of including magnetic correlations on the specific heat and uniform susceptibility. The details of the magnetic behavior and of the interaction of the charge and spin degrees of freedom will not be correctly given.

From the mean-field theory one finds that depending on the values of the parameters E_g, t_pE_g/t_{pd}, δ, and J the behavior may be characteristic of any of the regimes (conventional metal, Brinkman-Rice, heavy-fermion, or magnetic) previously discussed. To distinguish them it is convenient to consider two physical quantities, the Fermi-surface density of states N_0 and the quasiparticle plasma frequency ω_p^*. The quasiparticle plasma frequency is defined as follows: In a crystal at $T=0$ the optical conductivity $\sigma(\omega)$ will have a term proportional to $\delta(\omega)$. The coefficient of this term is $\omega_p^{*2}/4$.

For $E_g<E_g^c$, and J sufficiently small the model is metallic at half-filling: N_0 and ω_p^* are essentially independent of doping for $t_pE_g/t_{pd}^2<1$; for $t_pE_g/t_{pd}^2\gtrsim 1$ they remain independent of δ until δ grows large enough that the heavy-fermion regime is reached when the effective Kondo exchange $t_{pd}^2/(E_g+4\delta t_p)$ becomes comparable to the p-electron bandwidth t_p, upon which N_0 grows and ω_p^* shrinks rapidly with δ. With increasing δ the condition $N_0J\sim 1$ eventually becomes satisfied, and N_0 and ω_p cease to vary strongly with δ.

For $E_g > E_g^c$ and small δ the physics is controlled by the Mott transition that occurs at $\delta=0$. In this regime if J is negligible the physics is qualitatively similar to that described in Refs. 2 and 3: in particular, $N_0 \sim \delta^{-1}$ and $\omega_p^{*2} \sim \delta$. However, parameters are strongly renormalized from the Kotliar-Lee-Read (KLR) values if $t_p E_g / t_{pd}^2$ is nonzero. *A priori* one expects a nonzero t_p to have two competing effects. The direct oxygen-oxygen overlap provides an additional channel for particle motion; this effect tends to increase the velocity. However, as t_p is increased, the rigidity of the oxygen wave function is increased, as is the tendency toward heavy-fermion behavior; these effects tend to decrease the velocity. We find that v_F/δ is a decreasing function of $t_p E_g / t_{pd}^2$, except at very small values of this parameter. If $t_p E_g / t_{pd}^2 \gtrsim 1$, then at a finite $\delta \sim \frac{1}{4}\exp(-4t_p E_g / t_{pd}^2)$ the model crosses over smoothly into the heavy-fermion regime previously described. At sufficiently small δ the condition $N_0 J \sim 1$ becomes satisfied; the magnetic susceptibility ceases to vary strongly with δ while ω_p^{*2} remains proportional to δ as $\delta \to 0$. We believe this latter regime is relevant for the high-T_c materials.

III. SIMPLIFIED MODEL

In this section we consider a simple one-dimensional model which is to some extent tractable analytically. In a subsequent section we shall apply the insights gained from the study of the simplified model to the analysis of a more realistic two-dimensional model. The results obtained on the one-dimensional model will be qualitatively similar to those obtained on the two-dimensional model (although numerical factors will change) because we study these models with a mean-field approximation. Typically, the qualitative physics of mean-field theories is independent of dimensionality. Special features of one dimensional problems, such as power-law correlations, are missed by our mean-field theory.

We consider the one-dimensional Cu-O lattice shown in the lower part of Fig. 1, with one d orbital (at energy ε_d^0) on each O site and one p orbital (at energy ε_p) on each O site. We consider Cu-O (pd) and O-O (pp) hopping, as shown in the lower part of Fig. 1. The phases are appropriate for Cu $d_{x^2-y^2}$ and O_p orbitals.

We use a hole notation, so that the vacuum is the state in which all orbitals are fully occupied. We assume an infinite energy cost to doubly occupy the Cu site with holes. We introduce a slave boson b to represent a Cu site with no holes and Lagrange multiplier, $\lambda=(\varepsilon_d-\varepsilon_d^0)$ to enforce the constraint $n_d+n_b=1$. We treat b and ε_d as static mean-field parameters to be determined by extremizing the energy.

The mean-field Hamiltonian in k space is then

$$H=\sum_{k\alpha}\{\varepsilon_d d_{k\alpha}^\dagger d_{k\alpha}+\varepsilon_p p_{k\alpha}^\dagger p_{k\alpha} + [it_{pd} b \sin(ka/2) d_{k\alpha}^\dagger p_{k\alpha}+\text{H.c.}] + 2t_p \cos(ka) p_{k\alpha}^\dagger p_{k\alpha}\} + N(\varepsilon_d-\varepsilon_d^0)(b^2-1) . \quad (3.1)$$

Here N is the number of sites in the crystal.

We now simplify the problem further by defining a dimensionless momentum variable y via $y=ka/\pi$ (a is the lattice constant) and approximating

$$\cos ka = 1-2y \quad (3.2a)$$

$$\sin^2 ka/2 = y . \quad (3.2b)$$

The fermionic part of Eq. (3.1) defines a quasiparticle band structure with two energy bands,

$$E^{\pm}(y)=\tfrac{1}{2}(\varepsilon_p+\varepsilon_d+2t_p-4t_p y) \pm\tfrac{1}{2}[(\varepsilon_p+2t_p-4t_p y-\varepsilon_d)^2+4t_{pd}^2 b^2 y]^{1/2} . \quad (3.3)$$

The lowest-lying part of the lower band is at the zone edge, $y=1$.

The Fermi momentum y_F is given by

$$y_F=\tfrac{1}{2}(1-\delta) , \quad (3.4)$$

where the total number of holes is $(1+\delta)$.

The mean-field equations, determined by minimizing $\langle H \rangle$, may be written

$$1-b^2=\int_{y_p}^1 dy\,[1+(\varepsilon_p+2t_p-4t_p y-\varepsilon_d)/R] , \quad (3.5a)$$

$$E_g-(\varepsilon_p-2t_p-\varepsilon_d)=\int_{y_F}^1 dy\, 2t_{pd}^2 y/R(y) , \quad (3.5b)$$

$$R^2(y)=(\varepsilon_p+2t_p-4t_p y-\varepsilon_d)^2+4t_{pd}^2 b^2 y . \quad (3.6)$$

Here we have defined the important parameter

$$E_g=\varepsilon_p-2t_p-\varepsilon_d^0 . \quad (3.7)$$

E_g is the negative of the energy of the bare d level measured from the bottom of the oxygen band. In the one-dimensional (1D) model the lowest states in the oxygen band are at ε_p-2t_p. In the two-dimensional (2D) model they are at ε_p-4t_p [cf. Eq. (3.1)].

The integrals in Eqs. (3.5) may be performed analytically, yielding nonlinear equations that may be solved numerically. For example, Eq. (3.5b) becomes

$$E_g-(\varepsilon_p-2t_p-\varepsilon_d)=\frac{t_{pd}^2}{8t_p^2}[R(1)-R(y_F)] - \frac{\Gamma t_{pd}^2}{64t_p^3}\ln\frac{8t_p R(1)+32t_p^2+\Gamma}{8t_p R(y_F)+32t_p^2 y_F+\Gamma} ,$$

where $\Gamma=4t_{pd}^2 b^2-8t_p(\varepsilon_p+2t_p-\varepsilon_d)$. The logarithm, which is important when t_p is sufficient large, and is cut off by b^2 when $\varepsilon_p+2t_p-\varepsilon_p<0$, is a signature of the Kondo effect.

We have solved Eqs. (3.5) numerically for various parameter regimes. We discuss the solutions below. However, analytic solutions yielding considerable insight are possible in certain limits. We discuss these first.

At $\delta=0$ the model exhibits a Brinkman-Rice metal-insulator transition as E_g is increased to a critical value E_g^c. At the transition, $b^2 \to 0$. To determine E_g^c we ex-

pand Eqs. (3.5) for small b, assuming $\varepsilon_p - 2t_p - \varepsilon_d > t_{pd} b$. We show that the assumption is self-consistent at $\delta = 0$ for E_g sufficiently close to E_g^c. We have verified also that for $E_g \geq E_g^c$, solutions of Eqs. (3.5) with $\varepsilon_p - 2t_p - \varepsilon_d < 0$ or $t_{pd} b > \varepsilon_p - 2t_p - \varepsilon_d > 0$ do not exist.

By expanding Eq. (3.6a) with respect to b^2 one obtains

$$0 = Ab^2 + Bb^4$$

with $B > 0$ and

$$A = 1 - \int_{y_F}^{1} dy \frac{2t_{pd}^2 y}{(\varepsilon_p - \varepsilon_d + 2t_p - 4t_p y)^2} . \tag{3.8}$$

The Brinkman-Rice transition occurs when $A = 0$. This determines $\varepsilon_p - \varepsilon_d$. Substitution into (3.5b) evaluated at $b^2 = 0$ determines E_g^c. Further analytic progress is possible in the limits $t_p / t_{pd} \to 0$ and $t_p / t_{pd} \to \infty$.

In the former case,

$$\varepsilon_p - 2t_p - \varepsilon_d = \frac{\sqrt{3}}{2} t_{pd} - \tfrac{8}{9} t_p + \cdots ,$$

so that

$$E_g^c = \sqrt{3} t_{pd} - \tfrac{8}{9} t_p + \cdots .$$

In the latter case,

$$\varepsilon_p - 2t_p - \varepsilon_d = t_{pd}^2 / 2t_p + \cdots$$

and

$$E_g^c = \frac{t_{pd}^2}{t_p} \left[\ln \frac{2t_p}{t_{pd}} + 0.25 \right] + \cdots .$$

The variation of E_g^c with t_p at fixed t_{pd}, determined by solving Eqs. (3.5) numerically, is plotted in Fig. 2. It is evident that the curve interpolates smoothly between the two limits, with the crossover occurring at $t_p \sim t_{pd}$.

It is at first sight surprising that increasing t_p leads to a decrease in the minimum gap needed to stabilize the insulating state at $\delta = 0$. One might naively expect that increasing t_p from zero opens an additional channel for particle motion, thereby making the system more metallic. However, increasing t_p increases the stiffness of the O band, thereby reducing the energy to be gained by hybridizing with the Cu.

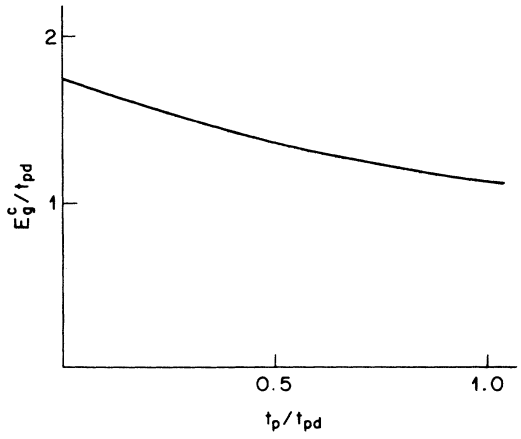

FIG. 2. Minimum gap E_g^c needed to stabilize insulating phase at half-filling plotted vs oxygen-oxygen hopping for one-dimensional model. Increasing t_p increases the energy cost of rearrangement of O orbitals needed to hybridize with Cu, hence renders the metallic state more difficult to sustain.

We next consider the behavior of the model for $E_g > E_g^c$ and $\delta > 0$. Now b^2 must vanish as $\delta \to 0$; in this case one must have $(\varepsilon_p - 2t_p - \varepsilon_d) > 0$, so that the quasiparticle level is below the bottom of the oxygen band. This may be understood by a simple argument. If one hole is added to the insulating state, then it must reside on the O site. In the absence of coupling to the Cu sites, the hole would reside in the bottom of the oxygen band. Within the mean-field theory, coupling to the Cu sites can only lower the energy of the quasiparticle. This is essentially the argument which Rice and Zhang[2] applied to the model with $t_p = 0$. Thus, for sufficiently small δ the quasiparticle states are pulled down below the oxygen band, independent of the value of t_p. However, the physical properties vary with t_p.

Consider first the limit $E_g \gg E_g^c$, $\delta \to 0$. For $t_p \ll t_{pd}^2 / E_g$ one has

$$\varepsilon_p - 2t_p - \varepsilon_d = \frac{3t_{pd}^2}{4E_g} - 8t_p / 9 , \tag{3.9a}$$

$$b^2 = \delta \left[\frac{3t_{pd}^2}{4E_g^2} - O(t_p E_g / t_{pd}^2)^2 \right] , \tag{3.9b}$$

$$v_F = \frac{\delta t_{pd}^2}{E_g} \left[1 + \frac{32}{27} \frac{t_p E_g}{t_{pd}^2} \right] . \tag{3.9c}$$

Recall that $E_g = \varepsilon_p - 2t_p - \varepsilon_d^0$ is the energy of the *bare d* level measured from the bottom of the oxygen band, and is also the gap in the insulating state. As t_p is increased at fixed E_g, the quasiparticle level moves closer to the oxygen band. For $t_p > t_{pd}^2 / E_g$ and $\delta \to 0$ we find

$$\varepsilon_p - 2t_p - \varepsilon_d = 2t_p \exp[-(2t_p E_g / t_{pd}^2)] , \tag{3.10a}$$

$$b^2 = \frac{4t_p^2 \delta}{t_{pd}^2} \exp \left[- \left[\frac{2t_p E_g}{t_{pd}^2} \right] \right] , \tag{3.10b}$$

$$v_F = 4t_p \delta \exp \left[- \left[\frac{2t_p E_g}{t_{pd}^2} \right] \right] , \tag{3.10c}$$

so that the quasiparticle level becomes exponentially close to the bottom of the p band. As t_p is increased from zero the Fermi velocity initially increases. This might be expected because direct oxygen-oxygen hopping opens an additional channel for particle motion. The increase in v_F shown in Eq. (3.9), however, occurs only for very small values of $(t_p E_g / t_{pd}^2) \lesssim 0.1$; for larger t_p values the decrease in b^2 begins to dominate and v_F ultimately vanishes exponentially with t_p; i.e., the quasiparticles become exponentially massive.

At sufficiently small δ, for both large and small t_p, we find $\varepsilon_p - 2t_p - \varepsilon_d > 0$ and $v_F \sim \delta$, indicating that the be-

havior is controlled by a Brinkman-Rice transition analogous to that in a one-band Hubbard model. This is the behavior expected from the Rice-Zhang arguments. The rapid decrease of the binding energy of the Rice-Zhang band with increasing t_p may be understood in terms of the rigidity argument used to justify the t_p dependence of E_g.

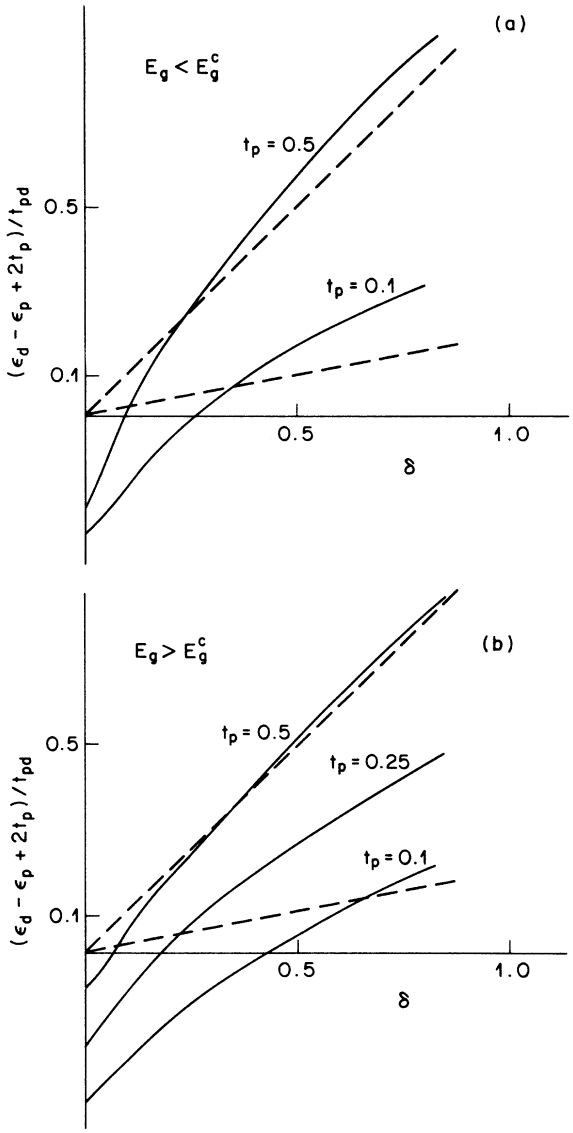

FIG. 3. Solid lines: quasiparticle energy level measured relative to bottom of oxygen band plotted vs doping. Dashed line: chemical potential of unhybridized oxygen band at doping δ. All calculations performed for 1D model. In (a), $E_g < E_g^c$ so the state is metallic at half-filling; in (b), $E_g > E_g^c$ so the state is insulating at half-filling. The heavy-fermion regime (quasiparticle resonance at energy slightly greater than chemical potential of unhybridized band) occurs for sufficiently large δ. For $E_g > E_g^c$, the heavy-fermion regime crosses over smoothly into the "Zhang-Rice" regime (bound state pulled out of oxygen band into insulating gap) for sufficiently small δ. Thus, there is no essential difference between a Zhang-Rice singlet and a heavy-fermion resonance.

However, for $t_p \geq t_{pd}^2/E_g$ and sufficiently large δ the behavior will no longer be governed by proximity to the Mott transition. We have already seen that $\epsilon_p - 2t_p - \epsilon_d$ decreases with increasing δ. For $t_p E_g/t_{pd}^2 > 1$, there exists a critical value of δ, δ_c, at which $\epsilon_p - 2t_p - \epsilon_d = 0$. For $\delta > \delta_c$ the Zhang-Rice band becomes a resonance in the oxygen band and as δ increases further, heavy-Fermion behavior results.

The critical value of δ may be estimated by equating the condensation energy per hole [ϵ_c, Eq. (3.14)] with the Fermi energy of the oxygen band with δ holes and $t_{pd} = 0$;

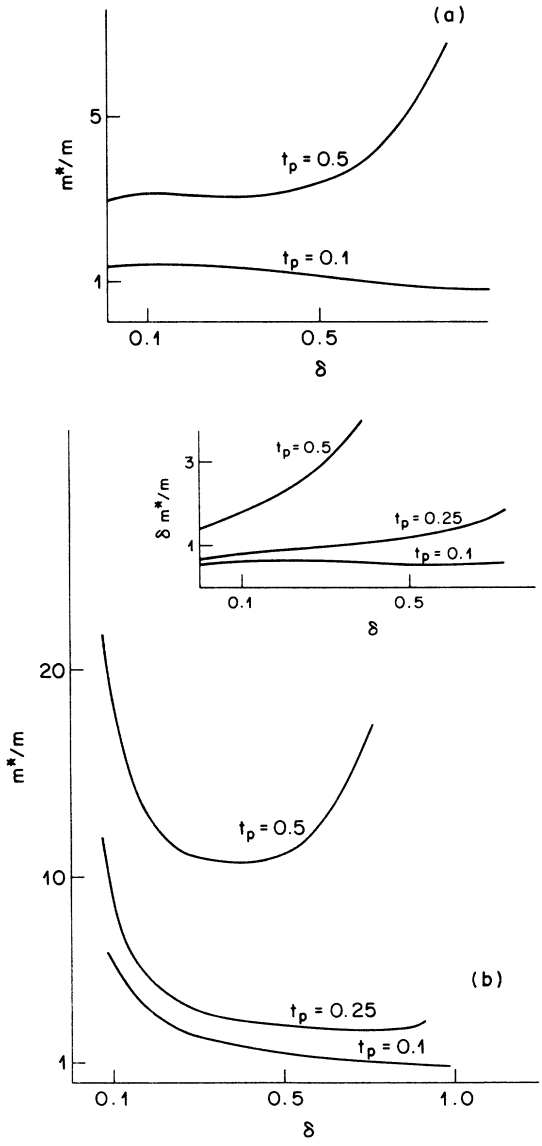

FIG. 4. Mass enhancements vs doping δ for $E_g < E_g^c$, metallic at half-filling (a) and $E_g > E_g^c$, insulating at half-filling (b). In (a) the onset of the heavy-fermion regime (exponentially large m^* exponentially dependent on δ) is evident for $t_p = 0.5$ at $\delta > 0.5$. In (b) the Brinkman-Rice behavior $m^*/m \sim \delta^{-1}$ (emphasized in the inset) is seen at small δ, and the heavy-fermion regime is seen at $\delta > 0.5$ for $t_p = 0.5$.

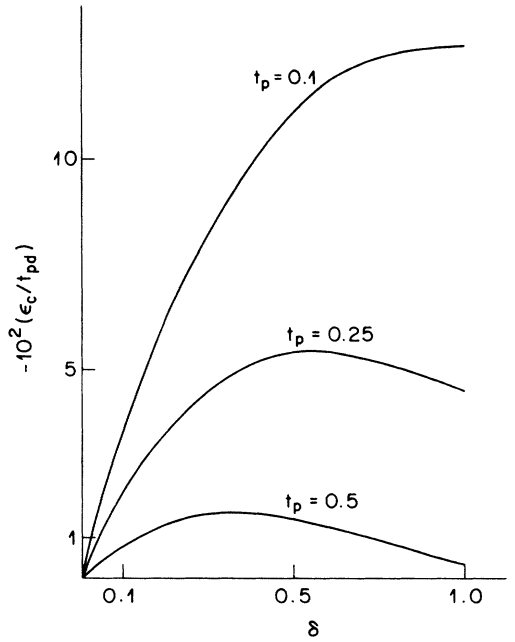

FIG. 5. Condensation energy ϵ_c vs doping δ for $E_g > E_g^c$, insulating at half-filling. E_c is the energy gained by coherent hybridization of O and Cu holes, and is the appropriate energy to compare with the magnetic ordering energy. Note the linear increase at small δ and the decrease, characteristic of the heavy-fermion regime, at large δ.

by solving Eqs. (3.5) under the condition $\epsilon_p - 2t_p - \epsilon_d = 0$ we find

$$\delta_c = \tfrac{1}{4}\exp\frac{-2t_p E_g}{t_{pd}^2} . \tag{3.11}$$

At $\delta = \delta_c$, $\epsilon_p - 2t_p - \epsilon_d = 0$ and

$$v_F = t_p \exp(-4t_p E_g / t_{pd}^2) . \tag{3.12}$$

Thus at the point $\delta = \delta_c$, the velocity is no longer proportional to δ and is indeed exponentially small. For $\delta > \delta_c$, v_F decreases further because the difference between the bare d level and the oxygen-band Fermi level increases.

To display the various regimes and crossovers in more detail we have solved the model numerically. The results are shown in Figs. 3–5.

Fig. 3 shows the energy of the quasiparticle level, $\epsilon_p - 2t_p - \epsilon_d$, as a function of δ at various values of t_p for the cases $E_g < E_g^c$ [Fig. 3(a)] and $E_g > E_g^c$ [Fig. 3(b)]. Figure 4 plots the mass enhancement m^*/m defined by

$$\frac{m^*}{m} = v^0/v^* . \tag{3.13}$$

Here v^0 is the unrenormalized velocity given by H [Eq. (1)] with $U^{dd} = 0$, i.e., with $b = 1$ and $\epsilon_d = \epsilon_d^0$. m^*/m measures the mass enhancement over this band structure value. It is also proportional to the inverse of the quasiparticle plasma frequency squared for this one-dimensional model. Figure 4(a) plots m^* versus δ at $E_g < E_g^c$. The rapid increase in m^* characteristic of the Kondo effect only occurs for large t_p and large δ. Figure 4(b) shows the mass enhancement for the case $E_g > E_g^c$. In the inset $(m^*\delta/m)$ is plotted to emphasize the Brinkman-Rice regime where $m^* \sim \delta^{-1}$. We note that marked deviations from the Brinkman-Rice behavior begin when $\delta \sim \delta_c$ if $t_p E_g / t_{pd}^2 \gtrsim 1$. The exponential rise characteristic of the Kondo effect does not begin until $2\delta t_p E_g / t_{pd}^2 \sim 1$. For the parameters considered we note that m^* increases with increasing t_p.

Figure 5 shows the condensation energy ϵ_c, for various parameters. ϵ_c is defined as

$$\epsilon_c = 2\int_{y_F}^{1} dy E^-(y) + (\epsilon_d - \epsilon_d^0)(b^2 - 1) - 2\int_{y_F}^{1} dy\,(\epsilon_p + 2t_p - 4t_p y) - \epsilon_d^0 . \tag{3.14}$$

ϵ_c is the energy per site relative to the energy of the unhybridized state with $b = 0$. A nonzero b indicates that the d electrons are coupled coherently to the p electrons, forming a Fermi liquid. ϵ_c is the energy gained by this process and is therefore the appropriate energy to compare with the magnetic ordering energy J. Note the increase of ϵ_c with increasing δ in the Mott regime and the rapid decrease of ϵ_c with increasing δ in the Kondo regime. When $\epsilon_c \lesssim J$ this theory is not applicable, because magnetic effects neglected in the theory become important.

A detailed treatment of the regime $\epsilon_c < J$ where magnetic correlation effects are important is an important unsolved problem in condensed-matter physics, and is beyond the scope of this paper. However, the qualitative effect of magnetic correlations upon the specific heat and susceptibility can be seen from a simple extension of our mean-field theory. We add to our Hamiltonian, Eq. (3.1), an explicit magnetic interaction term

$$J \sum_i \mathbf{S}_i \cdot \mathbf{S}_{i+1} . \tag{3.15}$$

Here $\mathbf{S}_i$ is the spin of a hole on Cu site i, $\mathbf{S}_i = d_{i\alpha}^\dagger \boldsymbol{\sigma}_{\alpha\beta} d_{i\beta}$ (explicitly including spins of holes on O sites would not change our results qualitatively). It is convenient to rewrite this term as

$$-\tfrac{1}{2}J \sum_{i\alpha} d_{i\alpha}^\dagger d_{i+1\alpha} d_{i+1\beta}^\dagger d_{i\beta} . \tag{3.16}$$

As shown, e.g., in Ref. 19, this interaction may be treated in mean-field theory by introducing various particle-hole and particle-particle expectation values. It is however very difficult to write down states with long-range magnetic order using this formalism. The predictions of the mean-field theory for phase diagrams of purely magnetic models [where the only terms in the Hamiltonian are magnetic terms such as (3.15)] have received substantial attention. Some work has also been done on the phase diagram and thermodynamics of one-band (t-J) models at nonzero δ. Discussing these complicated issues is beyond the scope of this paper. Here we wish simply to demonstrate that incorporating the magnetic coupling J provides a new energy scale, unrelated to ϵ_c, on which the spin entropy is quenched, so that in the regime $\epsilon_c \lesssim J$ the specific heat and uniform susceptibility do not depend

strongly upon δ or $\varepsilon_p-\varepsilon_d$. For this purpose consideration of any of the mean-field states suffices, and for simplicity we choose the uniform RVB state $\Delta_i=J\sum_\alpha \langle d^\dagger_{i\alpha}d_{i+1\alpha}\rangle=\Delta_0$. This state was shown[20] to be stable for small J and finite δ. The mean-field Hamiltonian then becomes

$$H=H_1+J_J \ , \tag{3.17}$$

where H_1 is given by Eq. (3.1) and

$$H_J=-\sum_k 2\Delta\cos(ka)d^\dagger_k d_k+2\Delta^2/J \ . \tag{3.18}$$

This extra term means that the quasiparticle energies $E^\pm$ [Eq. (3.3)] become

$$E^\pm(y)=\tfrac{1}{2}[\varepsilon_p+2t_p(1-2y)+\varepsilon_d-2\Delta(1-2y)] \pm\tfrac{1}{2}\{[\varepsilon_p+2t_p(1-2y)-\varepsilon_d+2\Delta(1-2y)]^2+4t_{pd}^2b^2y\}^{1/2} \ . \tag{3.19}$$

The mean-field equations are now determined by minimizing H with respect to ε_d, b, and Δ. They become

$$1-b^2=\int_{y_F}^1 dy\{1+[\varepsilon_p+2t_p(1-2y)-\varepsilon_d+2\Delta(1-2y)]/R^1\} \ , \tag{3.20a}$$

$$E_g-(\varepsilon_p-2t_p-\varepsilon_d)=\int_{y_F}^1 dy\ 2t_{pd}^2y/R^1 \ , \tag{3.20b}$$

$$\frac{4\Delta}{J}=+\int_{y_F}^1 dy((1-2y)\{1+[\varepsilon_p+2t_p(1-2y)-\varepsilon_d+2\Delta(1-2y)]/R^1\}) \ , \tag{3.20c}$$

with

$$[R^1(y)]^2=[\varepsilon_p+2t_p(1-2y)-\varepsilon_d+2\Delta(1-2y)]^2+4t_{pd}^2b^2y \ . \tag{3.21}$$

Consider the limit $E_g>E_g^c$, $t_{pd}^2>JE_g$, $t_p=0$ and $\delta\to 0$. Then an approximate analytic solution is easily found:

$$\varepsilon_p-\varepsilon_d=\frac{3t_{pd}^2}{4E_g}+O(J) \ , \tag{3.22a}$$

$$b^2=\delta\frac{3t_{pd}^2}{4E_g^2}+O(J/(\varepsilon_p-\varepsilon_d)) \ , \tag{3.22b}$$

$$\Delta=-J/8 \ , \tag{3.22c}$$

$$v_F=J/2+\delta t_{pd}^2/E_g \ . \tag{3.22d}$$

Thus we see explicitly in this limit that the Brinkman-Rice singularity in, e.g., the specific-heat coefficient $\gamma\sim v^{-1}$ is cut off by the magnetic effects so that $\gamma\sim J^{-1}$ as $\delta\to 0$.

One finds similar behavior in the heavy-fermion limit, with

$$v^*\simeq J/2+4t_p\exp(-2t_{pd}^2/t_pE_g) \ . \tag{3.23}$$

Again we emphasize that the mean-field theory is unlikely to represent correctly the detailed physics of the regime with $\varepsilon_c<J$, but it does demonstrate explicitly that the Brinkman-Rice and heavy-fermion singularities are cut off by magnetic effects at the energy scale J, although the coefficient of the term proportional to J in Eq. (3.22d) or (3.23) may not be correctly given.

IV. REALISTIC MODEL

In this section we present results for a more realistic two-dimensional model of the CuO_2 layers. In the notation of Fig. 1 the mean-field Hamiltonian is

$$H=\sum_{k\sigma}[(\varepsilon_d+2\Delta\beta_k)d^\dagger_{k\sigma}d_{k\sigma}-2t_{pd}b\sin(k_x/2)(d^\dagger_{k\sigma}p^x_{k\sigma}+\text{H.c.})-2t_{pd}b\sin(k_y/2)(d^\dagger_{k\sigma}p^y_{k\sigma}+\text{H.c.}) +\varepsilon_p(p^{x\dagger}_{k\sigma}p^x_{k\sigma}+p^{y\dagger}_{k\sigma}p^y_{k\sigma})-2t_p\alpha_k(p^{x\dagger}_{k\sigma}p^y_{k\sigma}+\text{H.c.})]+(\varepsilon_d-\varepsilon_d^0)(b^2-1)+2\Delta^2/J \ . \tag{4.1}$$

Here

$$\beta_k=\cos k_x+\cos k_y \ , \tag{4.2a}$$

$$\alpha_k=2\sin(k_x/2)\sin(k_y/2) \ . \tag{4.2b}$$

The self-consistency equations are obtained as described in the previous section. Again for the magnetic order parameter only the uniform RVB solution has been considered. The self-consistency equations have been solved numerically. The mean-field parameters b, Δ, and ε_d determine the quasiparticle band structure. From this,

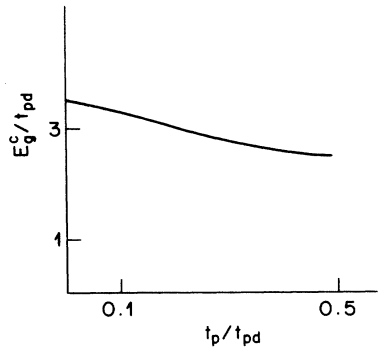

FIG. 6. Minimum gap E_g^c needed to stabilize insulating phase at half-filling plotted vs oxygen-oxygen hopping t_p for two-dimensional model. Increasing t_p increases energy cost for rearrangement of O orbitals needed to hybridize with Cu, hence renders metallic state more difficult to sustain.

the density of states and plasma frequency are computed.

As with the 1D model considered in the previous section the present model is an insulator at half-filling ($\delta=0$) if $E_g \equiv \varepsilon_p - 4t_p - \varepsilon_d^0$ is greater than a critical value E_g^c. Figure 6 shows the dependence of E_g^c on t_p, assuming $J=0$.

We have studied in detail two sets of parameters:

(I) $E_g=1.45$, $t_{pd}=1.3$, $t_p=0.9$, $J=0$;

(II) $E_g=10.4$, $t_{pd}=1.3$, $t_p=0.7$, $J=0$.

The parameter set (I) was chosen on the basis of local-density calculations.[21,22] From Fig. 6 it is clear that for these parameters the system is metallic at half-filling. The parameter set (II) was chosen to force the system to be insulating at half-filling. All of the energies are measured in eV.

For each parameter set we have computed the quasiparticle density of states N_0 and plasma frequency ω_p^*. For our 2D CuO_2 model with $J=0$ these are defined as

$$N_0 = 2\sum_k \delta(E_k^- - \mu) , \tag{4.3a}$$

$$\frac{\omega_p^{*2}}{4\pi} = 2\sum_k \left[\frac{\partial E_k^-}{\partial k_x}\right]^2 \delta(E_k^- - \mu) , \tag{4.3b}$$

where E_k^- is the dispersion relation of the lowest quasiparticle band defined by Eq. (4.1).

We choose, however, to present our results in dimensional units to facilitate comparison with experiment. N_0 is already given from Eq. (4.3a) in units of states/planar Cu eV given the choice of parameters above. To obtain the physical plasma frequencies we must multiply ω_p^{*2} from Eq. (3b) by $4\pi e^2/d$, where e is the charge of the electron and d is the distance between CuO_2 planes. For $YBa_2Cu_3O_{5+x}$, $d=6.6$ Å. The numerical results should be treated with caution, however, for in addition to the errors introduced by the mean-field approximation, uncertainty due to the tight-binding parametrization of the band structure is also present. The tight-binding fit to the band structure may be recovered by setting $b=1$ and $\varepsilon_p - \varepsilon_d < t_{pd}$. We find that the density of states and plasma frequency may vary $\sim 50\%$ depending on the precise values assumed for $\varepsilon_p - \varepsilon_d$ and t_p. We believe that this variation is due to the presence, in the band calculation, of a van Hove singularity whose precise position depends sensitively on $\varepsilon_p - \varepsilon_d$ and t_p. We note, e.g., that the Hybertsen-Christiansen-Schluter (HCS)[21] parameters $\varepsilon_p - \varepsilon_d \sim 1$ eV, $t_{pd} \sim 1.3$ eV, $t_p \sim 0.5$ eV lead at $\delta=0$ to $N_0 \sim 1.3$/eV and $\omega_p^2 \sim 13$ eV^2, which are to be compared with the values $N_0 \sim 1.2$/eV and $\omega_p^2 \sim 10$ eV^2 obtained directly from local-density calculations. Because the HCS parameters put the van-Hove singularity at $\delta=0.23$ rather than at $\delta=0.15$ as the local-density-approximation (LDA) calculations do, the discrepancy with the LDA N_0 will increase as δ is increased from zero. The discrepancy between the tight binding fit and the actual band structure will presumably propagate into the results of our mean-field calculation, leading to some uncertainty in our values for physical parameters.

The results for the density of states and plasma frequency as a function of doping, δ, are shown in Figs. 7 and 8. Figure 7 presents the results for parameter set (I), which leads to metallic behavior at half-filling. The van Hove singularity at $\delta \sim 0.3$ may be seen in N_0. Note that although correlation effects enhance N_0 and reduce ω_p^* from the band-structure values, there is no strong doping dependence. Note also that the heavy-fermion regime discussed in the previous section is not reached, although t_p has been chosen to be rather large.

Figure 8 presents results for parameter set (II), which leads to insulating behavior at half-filling. The solid line

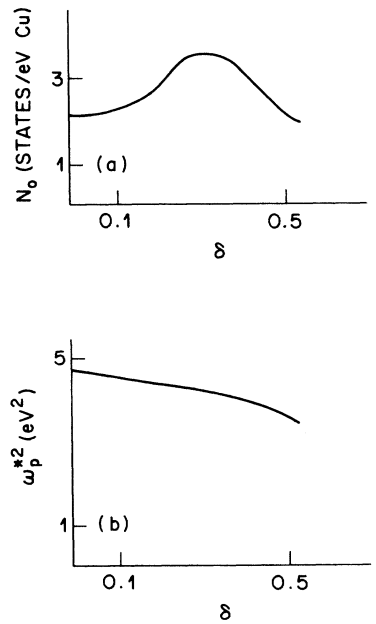

FIG. 7. Density of states N_0 (a) and squared quasiparticle plasma frequency ω_p^{*2} (b) plotted vs doping δ for two-dimensional model using parameters determined (Ref. 21) from local-density calculations. For these parameters, the model is metallic at half-filling, in contrast to experiment.

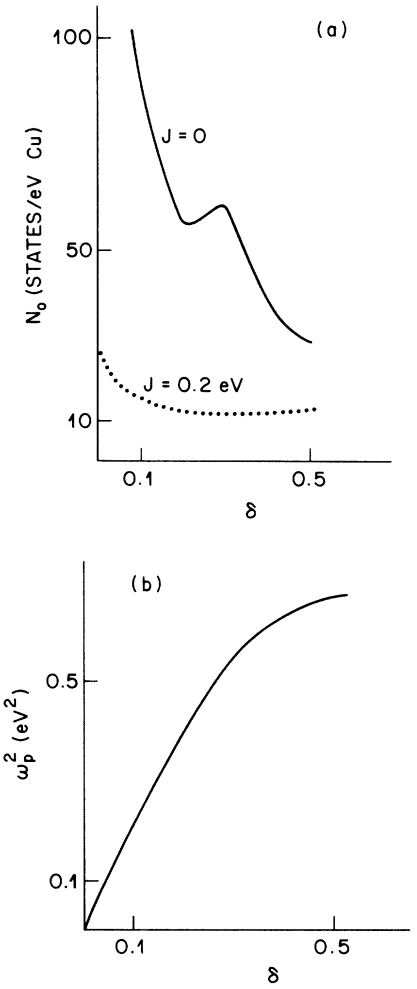

FIG. 8. Density of states N_0 (a) and squared plasma frequency ω_p^{*2} (b) plotted vs doping δ for two-dimensional model using hybridization parameters determined (Ref. 21) from local-density calculations, but a *p-d* splitting $E_g = 10.4$ eV chosen large enough to force the system to be insulating at half-filling. The solid line in (a) shows the Brinkman-Rice divergence in N_0 as $\delta \to 0$, for the model without magnetic correlations. The dotted line shows the effect of magnetic correlations, which eliminate the divergence as $\delta \to 0$. The plasma frequency shown in (b) varies with δ in a manner consistent with experiment, but comparison with Table I shows that the magnitude is too small.

in Fig. 8(a) shows the density of states. The strong δ dependence is evident, as is the van Hove singularity at $\delta \sim 0.3$. The dotted line in Fig. 8(a) shows the density of states for the same parameters but with $J = 0.2$ eV. The dramatic effect of including magnetic correlations is evident: the magnitude and δ dependence are much reduced. In particular, N_0 has a finite limit as $\delta \to 0$. In Fig. 8(b) the square of the quasiparticle plasma frequency is shown, for the same parameters as the solid line in Fig. 8(a). The noteworthy features are the linear δ dependence at low δ and the very small overall magnitude.

V. EXPERIMENTAL EVIDENCE

In this section we attempt to determine which of the various parameter regimes previously described is appropriate for the high-T_c superconductors by analyzing the magnitude and doping dependence of the optical conductivity, susceptibility, and specific heat. We argue that the spectral weight in the quasiparticle contribution to the optical conductivity scales with the doping δ, as expected if the physics is controlled by proximity to a Mott transition. However, available information suggests that the conduction-electron contribution to the specific heat and susceptibility remains relatively constant, independent of doping. Within the mean-field theories we have considered this behavior can only be reconciled with the optical data if magnetic correlations are important.

We turn now to a discussion of the optical experiments. It is known that high-T_c superconductors are created by doping antiferromagnetic insulating "parent compounds." However, it has never been clearly established where the parent compounds lie on the continuum ranging from weakly coupled spin-density-wave systems to strongly coupled Mott insulators. On a bipartite lattice we believe that no sharp transition distinguishes the two types of insulator. There is, however, a crossover between the spin-density-wave case where the presence of magnetic order is necessary to obtain the insulating behavior and the Mott regime where correlation effects lead to insulating behavior whether or not the magnetic moments are ordered.

One way to address the issue is to compare the optical gap E_g in the insulating state with the critical value E_g^c at which the metallic Fermi-liquid solution to the mean-field theory vanishes. E_g^c sets the scale for crossover from band to Mott behavior. An alternative is to consider the doping dependence of the physical properties of the system. In particular, the mobile-carrier plasma frequency squared should scale with the number of dopants in the Mott case, even when the material is no longer magnetically ordered, while in the spin-density-wave case the effective plasma frequency should revert to essentially the band-theory value immediately upon the destruction of the magnetic order.

The experimental value for E_g is difficult to determine with certainty. Optical reflectivity measurements should show a feature at E_g. However, the results of the previous section indicate that the lowest direct interband transition has a vanishing optical matrix element, so that the feature at E_g is very soft. Pure stoichiometric La_2CuO_4 is difficult to obtain. Presently available optically studied samples of La_2CuO_4 have a large concentration of defect states that cause subgap absorption and, presumably, broadening of the edge at E_g. The apparent gap edge is at $E_g \sim 1.5$ eV.[23] The related compound Nd_2CuO_4 (which has similar structure but with Cu fourfold instead of sixfold coordinated with O) can be made with fewer defects. It exhibits an optical gap at $E_g \sim 1.5$ eV.[23,24] At the gap edge a sharp feature occurs; this feature has been attributed to an exciton. Both excitons and lifetime broadening due to defects tend to reduce the observed gap; thus the optical experiments on Nd_2CuO_4 and La_2CuO_4 indicate $E_g \gtrsim 1.5$ eV. In $YBa_2Cu_3O_{6.0}$ significant absorption begins to appear at 1.7 eV,[25] again with structure at the gap edge. The structure is less sharp and is of less spectral weight than that in

Nd_2CuO_4. The origin of the structure is not understood; in particular it is not known whether it is associated with the CuO_2 planes. However, because the absorption at $\omega < 1.7$ eV is small, the data suggest $E_g \geq 1.7$ eV in this material. Other measurements of the dynamics of photoexcited carriers in La_2CuO_4 (Ref. 26) also point to a gap of ~ 2 eV, although with larger uncertainties.

One would like to compare the experimental E_g to the theoretically determined crossover scale E_g^c. Unfortunately, E_g^c depends upon the parameters t_{pd} and t_p which are more difficult to determine from experiment. Accepting the values proposed, e.g., by Hybertsen, Christiansen, and Schluter,[21] $t_{pd} = 1.3$ and $t_p = 0.65$ eV, and using the results in Fig. 6 puts the system in the regime $E_g < E_g^c$, i.e., in the metallic regime at $\delta = 0$. This analysis would suggest that the observed insulating behavior at $\delta = 0$ is due to the magnetic ordering. However, the large value of the gap and the scaling of the quasiparticle spectral weight with doping argue against this possibility.

We now consider the variation of the optical conductivity with doping. In the mean-field theories discussed previously the optical conductivity $\sigma(\omega)$ has the form

$$\sigma(\omega) = \frac{\omega_p^{*2}}{4}\delta(\omega) + \text{interband terms} . \tag{5.1}$$

The term concentrated at zero frequency is the effective mobile carrier contribution to σ. The spectral weight in this contribution is given by $\frac{1}{8}\omega_p^2$. In a more realistic model other interactions not included in the mean-field theory will remove weight from the δ function. It is reasonable, however, to expect that these other interactions will have a strength that is roughly independent of doping.

The interband terms are of two sorts. One is the interband transition from the bare d level to the p band. This transition should occur at an energy of order E_g possibly corrected by excitonic effects. The other is a low-lying interband transition predicted by the mean-field theory. It has been discussed in the context of heavy-electron metals[9] and high-temperature superconductivity,[3] but it is not well understood theoretically. In this paper we have calculated only ω_p^* for which, we believe, the mean-field theory provides a reasonable estimate. A subsequent paper will contain a more complete discussion of $\sigma(\omega)$.

We now consider the available data. One useful measurement for superconducting samples is of the $T = 0$ value of the London penetration depth, which yields the superfluid density. This is the coefficient of a term proportional to $\delta(\omega)$ in the optical conductivity of a superconductor. It thus defines a renormalized plasma frequency ω_p^R. In the context of the mean-field theories, ω_p^R is to be interpreted of as the mobile-carrier plasma frequency ω_p^*, reduced by mass renormalizations due to other interactions not included in the mean-field theory.

Another important class of measurements is infrared and optical reflection and transmission. From these experiments the full $\sigma(\omega)$ may in principle be determined and the mobile-carrier contribution extracted. In practice, accurate data over a sufficiently wide frequency range are only available for the $YBa_2Cu_3O_{7-\delta}$ system, although some data are available for the Bi-Ca-Sr-Cu-O and $La_{2-x}Sr_xCuO_4$ systems. Extraction of the interesting mobile-carrier contribution to σ is hampered by the lack of a theoretically determined functional form for this contribution, and its possible overlap with interband transitions and the presence, in the YBa system at least, of additional absorption apparently unrelated to the CuO_2 planes.

Analysis of reflectivity and penetration-depth data in

TABLE I. Variation of Physical Properties of Cuprate Superconductors with Doping. Column one identifies the material and column two gives an estimate of the doping. For $La_{2-x}Sn_xCuO_4$ we assume $\delta = x$. For the YBa materials we estimate δ from valence counting arguments similar to those used in Ref. 27. The uncertainties in δ are large, but the trend is clear. Column three gives the quasiparticle plasma frequencies obtained from penetration depth (Ref. 28) or optical (Ref. 29) measurements. Column four gives the density of states N_0^γ per planar copper (Cu_{II}) inferred from the specific-heat coefficient γ, which is estimated by applying the BCS relation to the measured (Refs. 30 and 31) specific-heat jump. Column five gives the density of states per planar copper (Cu_{II}) inferred from the measured (Refs. 32 and 33) magnetic susceptibility, corrected for van Vleck and core diamagnetism. For $La_{1.85}Sr_{0.15}CuO_4$ we assumed $\chi_{obsd} = \chi_{Pauli} - 75\times10^{-6}$ cm^3/mol Cu (Ref. 34) and for $YBa_2Cu_3O_{6+x}$ we assumed $\chi_{obsd} = \chi_{Pauli} - 46\times10^{-6}$ cm^3/mol Cu II (Ref. 35). We emphasize that ω_p^* is well established, and although the numbers for δ and N_0 are not as well determined, the trends with doping are clear.

Material	δ	ω_p^{*2} (eV^2)	N_0^γ (eV^{-1}/Cu II)	N_0^χ (eV^{-1}/Cu II)
$La_{1.85}Sr_{0.15}CuO_4$	0.15	1.1	5	2–2.5
$YBa_2Cu_3O_{6+x}$ ($T_c = 30$)	0.03–0.07	0.5		
$YBa_2Cu_3O_{6+x}$ ($T_c = 50$)	0.1–0.2	1.0		2.5–3.5
$YBa_2Cu_3O_{6+x}$ ($T_c = 80$)	0.2–0.3	1.8		4
$YBa_2Cu_3O_{6+x}$ ($T_c = 90$)	0.3–0.5	2.3	8–9	4–5
Band theory CuO_2 plane at half-filling	0	9.0	1.2	1.2

the YBa system is also complicated by lack of precise information concerning the doping of the samples. The available data are nevertheless collected in Table I.

The first column describes the material, the second column gives an estimate of the doping. The third column gives the spectral weight in the $\omega \to 0$ δ-function contribution; this is to be compared with the quantity ω_p^{*2} calculated in Sec. IV. We have scaled the experimental plasma frequencies by the ratio of the distance between CuO_2 planes in the relevant material to that in La_2CuO_4 so that plasma frequencies for different materials may be compared with each other, with band structure calculations for La_2CuO_4, and with our results.

Despite the uncertainties it is clear that the low-frequency spectral weight associated with mobile carriers on the CuO_2 planes increases as the doping increases, and that the spectral weight per dopant is large.

We now consider the specific-heat coefficient γ and the conduction-electron contribution to the magnetic susceptibility. The specific-heat coefficient cannot be determined unambiguously in the cuprate superconductors because of their high transition temperatures. We have obtained the values for γ given in column four of Table I from the measured specific-heat jumps at the superconducting transition by assuming the BCS relation $\Delta C = 1.43\gamma T_c$. We have obtained the estimates of the Pauli susceptibility in column five of Table I by correcting the measured susceptibility for core diamagnetism and van Vleck terms as described in the table caption. We have expressed the results in units of states/planar Cu eV, again allowing easy comparison of different materials.

Compare the experimental results for N_0 and ω_p^{*2} with the theoretical results given in Figs. 7 and 8. The variation with doping of the plasma frequency suggests that the high-T_c materials are in the regime $E_g > E_g^c$ in which there is Mott insulating behavior at half-filling. The relative absence of variation in the specific heat and susceptibility density of states suggests that the materials are in a regime in which magnetic correlations dominate the thermodynamics (as shown, e.g., in the dotted line in Fig. 8). However, the relatively large value of the plasma frequency is difficult to account for within mean-field theory. Indeed, if parameters are tuned to produce an $\omega_p^{*2} \sim \delta$ for $\delta < 0.4$, say, the ratio ω_p^{*2}/δ will be too small compared with the experimental value. It is possible that a fine-tuning of parameters such as t_p, or that a better understanding of the effects of the nearest-neighbor repulsion will resolve this problem, but as of this writing it appears that the mean-field theory provides a qualitatively but not quantitatively accurate account of the doping dependence of ω_p^*.

VI. CONCLUSION

We have considered mean-field theories of the CuO_2 planes believed to be responsible for high-temperature superconductivity. We have discussed the various regimes of behavior and the crossovers between them, and have compared the results of the mean-field theories with experiment. The qualitative behavior suggests that the physics is controlled by proximity to a Mott transition and that a theory which includes intersite magnetic correlations is essential. The oxygen-oxygen hybridization is apparently not large enough to produce heavy-fermion behavior at any reasonable doping.

Several important quantitative questions remain. One is that if both the mean-field theory and the model parameters proposed on the basis of local-density calculations were accurate, La_2CuO_4 would not be a Mott insulator at half-filling. Another is that if the model parameters are adjusted to produce insulating behavior, the theoretical quasiparticle plasma frequencies are too low relative to the observed plasma frequencies. However, the difference is not unreasonably large, the numerical accuracy to be expected from the mean-field theory is not known, and effects of the intersite Coulomb interaction V are not well understood.

Note added in proof. Recently, more accurate estimates of the planar spin susceptibility for $YBa_2Cu_3O_{6+x}$ have become available from analysis of Knight-shift measurements.[36,37] These estimates are $N_0^\chi(\text{eV}^{-1}/\text{Cu II}) = 2.5-3$ (for $YBa_2Cu_3O_7$) and $N_0^\chi(\text{eV}^{-1}/\text{Cu II}) = 0.5-1$ (for $YBa_2Cu_3O_{6.6}$ at $T = 100$ K). These new estimates strengthen the conclusions of Sec. V that the enhancement over band theory of the susceptibility is much less than that of the quasiparticle plasma frequency and scales oppositely with doping.

ACKNOWLEDGMENTS

We are grateful to Dr. M. Hybertsen for discussion of the band-structure calculations and of the extraction of tight-binding and interaction parameters from them. Some of the work reported here was performed at the Aspen Center for Physics. One of the authors (A.J.M.) performed some of the work reported here during a visit to the Institute for Theoretical Physics, Santa Barbara, where he was supported in part by the National Science Foundation (NSF) under Grant No. PHY 82-17853, supplemented by funds from the National Aeronautics and Space Administration. One of us (B.G.K.) acknowledges NSF Grant No. DMR 8657557. Much of this work was performed while the authors were at MIT.

APPENDIX

In this appendix we demonstrate that including the nearest-neighbor repulsion V introduced in the high-T_c problem by Varma, Schmitt-Rink, and Abrahams[12] leads in the mean-field theory only to an increase of the effective gap energy E_g.

We add to our Hamiltonian, Eq. (2.1), an extra term

$$H_V = \frac{V}{N} \sum_{i\eta\sigma} d_{i\sigma}^\dagger d_{i\sigma} c_{i+\eta,\sigma}^\dagger c_{i+\eta\sigma} \ . \tag{A1}$$

Here η labels the nearest-neighbor O sites of Cu site i, N is the number of unit cells in the crystal, and V is the interaction.

Treating this term in mean-field theory leads to extra terms in the mean-field Hamiltonian, Eq. (4.1). Denoting these extra terms H_V^{MF} we have

$$H_V^{\mathrm{MF}} = 2v_0 \sum_{i\sigma} c^\dagger_{i+x\sigma} c_{i+x\sigma} + c^\dagger_{i+y\sigma} c_{i+y\sigma} - 4v_0^* \sum_{i\sigma} d^\dagger_{i\sigma} d_{i\sigma} + \frac{8N}{V} v_0 v_0^* \ . \quad \text{(A2)}$$

Here

$$v_0 = \frac{1}{2N} V \sum_{i\sigma} \langle d^\dagger_{i\sigma} d_{i\sigma} \rangle \ , \quad \text{(A3a)}$$

$$v_0^* = -\frac{1}{4N} V \sum_{i\sigma} \langle c^\dagger_{i+x\sigma} c_{i+x\sigma} \rangle + \langle c^\dagger_{i+y\sigma} c_{i+y\sigma} \rangle \ , \quad \text{(A3b)}$$

and these mean-field parameters are determined by minimizing H with respect to ε_d, b, Δ, v_0, and v_0^*.

It is evident that the role of v_0 and v_0^* is to shift the energies of the p and d levels to $\tilde{\varepsilon}_p = \varepsilon_p + 2v_0 > \varepsilon_p$ and $\tilde{\varepsilon}_d = \varepsilon_d - 4v_0^* > \varepsilon_d$. However, for small doping, $\langle c^\dagger c \rangle \sim \delta$ while $\langle d^\dagger d \rangle \sim 1$, so that for $\delta \ll 1$ the d level is shifted much less than the p level and the effect of V is to increase the splitting and thus to favor insulating behavior.

[1]See, e.g., D. van der Marel, J. van Elp, G. A. Sawatzky, and D. Heitman, Phys. Rev. B **37**, 5136 (1988).

[2]T. M. Rice and F. C. Zhang, Phys. Rev. B **37**, 3754 (1988).

[3]B. G. Kotliar, P. A. Lee, and N. Read, Physica C **153-155**, 538 (1988).

[4]W. F. Brinkman and T. M. Rice, Phys. Rev. B **3**, 4302 (1970).

[5]B. I. Shraiman and E. D. Siggia, Phys. Rev. Lett. **60**, 740 (1988).

[6]C. L. Kane, P. A. Lee, and N. Read, Phys. Rev. B **39**, 6880 (1989).

[7]S. Schmitt-Rink, C. M. Varma, A. E. Ruckenstein, Phys. Rev. Lett. **60**, 2793 (1988).

[8]N. Read, D. M. Newns, and S. Doniach, Phys. Rev. B **30**, 3891 (1984).

[9]A. J. Millis and P. A. Lee, Phys. Rev. B **35**, 3394 (1987).

[10]A. Auerbach and K. Levin, Phys. Rev. Lett. **57**, 877 (1986).

[11]S. Doniach, Physics **91B**, 231 (1977).

[12]C. M. Varma, S. Schmitt-Rink, and E. Abrahams, Solid State Commun. **62**, 681 (1987).

[13]D. M. Newns, M. Rasolt, and P. C. Patinaik, Phys. Rev. B **38**, 6513 (1988).

[14]C. A. Balsiero, M. Avignon, A. G. Rojo, and B. Alascio, Phys. Rev. Lett. **62**, 2624 (1989).

[15]Ju. H. Kim, K. Levin, and A. Auerbach, Phys. Rev. B **39**, 11 633 (1989); and (unpublished).

[16]C. Castellani and B. G. Kotliar, Phys. Rev. B **39**, 2876 (1989).

[17]S. E. Barnes, J. Phys. F **26**, 1375 (1976).

[18]N. Read, J. Phys. C **18**, 2651 (1985); P. Coleman, Phys. Rev. B **29**, 3035 (1984).

[19]G. Baskaran, Z. Zou, and P. W. Anderson, Solid State Commun. **63**, 973 (1987); I. Affleck and J. B. Marston, Phys. Rev. B **37**, 3774 (1988); B. G. Kotliar, *ibid.* **37**, 3664 (1988).

[20]M. Grilli and B. G. Kotliar, Phys. Rev. Lett. **64**, 1170 (1990).

[21]M. Hybertsen, N. E. Christiansen, and M. Schluter, Phys. Rev. B **39**, 9028 (1989).

[22]A. K. McMahan, R. M. Martin, and S. Satpathy, Phys. Rev. B **38**, 6650 (1989).

[23]S. Tajima, H. Ishii, T. Nakahashi, T. Takagi, S. Uchida, M. Seki, S. Suga, Y. Hidaka, M. Suzuki, T. Murakami, K. Oka, and H. Unoki, J. Opt. Soc. Am. B **6**, 475 (1989).

[24]S. L. Cooper, G. A. Thomas, J. Orenstein, D. H. Rapkine, A. J. Millis, S.-W. Cheong, A. S. Cooper, and Z. Fisk, Phys. Rev. B (to be published).

[25]J. Orenstein, G. A. Thomas, D. H. Rapkine, A. J. Millis, L. F. Schneemeyer, and J. V. Waszczak, Physica C **153-155**, 1740 (1988).

[26]J. M. Ginder, M. G. Roe, Y. Song, R. P. McCall, J. R. Gaines, E. Ehrenfreund, and A. J. Epstein, Phys. Rev. B **37**, 7506 (1988).

[27]Y. Tokura, J. B. Torrance, T. C. Huang, and A. I. Nazzal, Phys. Rev. B **38**, 7156 (1988).

[28]D. R. Harshman, L. F. Schneemeyer, J. V. Waszczak, G. Aeppli, R. J. Cava, B. Batlogg, L. W. Ropp, E. J. Ansaldo, and D. L. Williams, Phys. Rev. B **39**, 851 (1989).

[29]J. Orenstein, G. A. Thomas, A. J. Millis, S. L. Cooper, D. H. Rapkine, T. Timusk, L. F. Schneemeyer, and J. V. Waszczak (unpublished).

[30]Junod *et al.*, Jpn. J. Appl. Phys. **26**, 1119 (1987).

[31]Junod *et al.*, Physica C **152**, 50 (1988).

[32]L. F. Schneemeyer, J. V. Waszczak, E. A. Rietman, and R. J. Cava, Phys. Rev. B **35**, 8421 (1987).

[33]D. C. Johnston *et al.*, Physica C **153-155**, 572 (1988).

[34]D. C. Johnston, Phys. Rev. Lett. **62**, 957 (1989).

[35]F. Mila and T. M. Rice, Physica C **157**, 561 (1989).

[36]R. E. Walstedt and W. W. Warren, Science (to be published).

[37]A. J. Millis, H. Monien, and D. Pines, Phys. Rev. B (to be published).